

Fig. 1 Receiver cylinder pressure.

taken to be the same for each receiver cylinder namely,  $P_0$ ,

$$P_1^n - \alpha P_1^{n-1} = (1 - \alpha)P_0 \quad (3)$$

The solution to the difference equation for this case is

$$P_1^n = (P^0 - P_0)\alpha^n + P_0 \quad (4)$$

For  $m = 2$ , an array of two supply vessels,

$$P_2^n - \alpha P_2^{n-1} = (1 - \alpha)P_1^n \quad (5)$$

combining Eqs. (4) and (5)

$$P_2^n - \alpha P_2^{n-1} = (1 - \alpha)[(P^0 - P_0)\alpha^n + P_0] \quad (6)$$

the solution of Eq. (6) is

$$P_2^n = (P^0 - P_0)\alpha^n[1 + n(1 - \alpha)] + P_0 \quad (7)$$

In a similar fashion the solutions for  $m = 3, 4$ , etc. can be found and by mathematical induction the general solution is found as

$$\frac{P_m^n - P_0}{P^0 - P_0} = \alpha^n \sum_{i=1}^m \frac{(n + i - 2)!}{(n - 1)!(i - 1)!} (1 - \alpha)^{i-1} \quad (8)$$

This expression yields the pressure of any supply vessel ( $m$ ) at any stage of its use ( $n$ ) and the pressure of any of the receiver vessels ( $n$ ) at any stage of the charging procedure ( $m$ ).

Figure 1 shows  $(P_m^n - P_0)/(P^0 - P_0)$  vs supply vessel number ( $m$ ) with the receiver vessel number ( $n$ ) as a parameter for  $\alpha = 0.75$ . For the particular volume ratio considered, this graph can be used to determine the pressure in any one of the receiver vessels ( $n$ ) after having been charged from some number of supply vessels ( $m$ ). Alternatively, this figure gives the pressure of any supply vessel ( $m$ ) as a function of the number of times it has been used ( $n$ ).

We can define the gas utilization efficiency  $\eta$  as the amount of gas removed from a supply vessel before it is taken out of

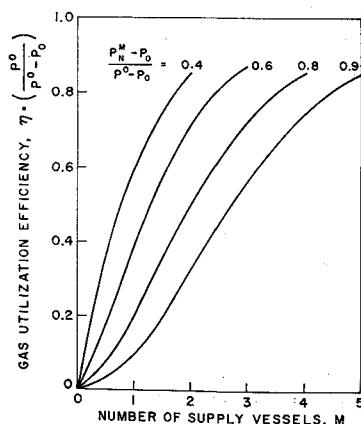


Fig. 2 Gas utilization efficiency.

the array compared to its initial content of gas

$$\eta = \frac{(P^0 - P_1^N)/P^0}{(P^0 - P_0)/P^0[1 - (P_1^N - P_0)/(P^0 - P_0)]} \quad (9)$$

where  $P_1^N$  is the pressure of the first supply vessel in the array when it is removed. This vessel is removed when the pressure in the last vessel in the array has dropped below the minimum required pressure of a receiver vessel. This minimum required pressure will be denoted by  $P_M^N$  and the number of the last supply cylinder in the array by  $M$ . From Eq. (8)

$$\frac{P_M^N - P_0}{P^0 - P_0} = \alpha^N \sum_{i=1}^M \frac{(N + i - 2)!}{(N - 1)!(i - 1)!} (1 - \alpha)^{i-1} \quad (10)$$

and

$$(P_1^N - P_0)/(P^0 - P_0) = \alpha^N \quad (11)$$

where  $N$  is the number of receiver vessels that have been charged when it becomes necessary to remove the first supply vessel and add a fresh one to the end of the array. In theory it is possible to solve Eq. (10) for  $N$  and using that value of  $N$  calculate  $P_1^N$  from Eq. (11) and thus determine the efficiency  $\eta$  from Eq. (9). However, this cannot be done, since Eq. (10) is transcendental in  $N$ .

It is possible to determine the gas utilization efficiency by what amounts to a graphical solution of Eqs. (10) and (11). Returning to Fig. 1 it can be seen that the pressure in the first supply vessel ( $m = 1$ ) can be read from the figure for the same number of uses at which the pressure in last supply vessel reaches  $P_M^N$ . This technique has been applied to Fig. 1 and the results are shown in Fig. 2 where the efficiency  $\eta[(P^0 - P_0)/(P_M^N - P_0)]$  is plotted as a function of the number of supply vessels in the array  $M$  for a number of values of the minimum required receiver pressure  $(P_M^N - P_0)/(P^0 - P_0)$ .

The following conclusions can be drawn from the results shown in Fig. 2. 1) Gas utilization efficiency increases rapidly with increased number of supply vessels. 2) A lower minimum required final pressure for the receiver vessels leads to a higher efficiency. 3) The number of supply cylinders required to obtain a given efficiency increases with increasing minimum required final pressure.

## Bondline Temperature of a Two-Layer Slab Subjected to Aeroheating—Graphical Solution

HERBERT J. HARRIS\*

TRW Systems Group, Houston, Texas

### Nomenclature

$c_p$	= specific heat at constant pressure, Btu/lb-°F
$F_0$	= dimensionless time (Fourier modulus), $\alpha\theta/l^2$ ;
	$F_{0f}$ = value ( $\alpha\theta_f/l^2$ ) at which the bondline temperature is to be determined
$f(x, \theta)$	= $T(x, \theta)$ (temperature as function of depth and time), °F
$f'$	= $\partial T / \partial F_0$ , °F
$f'(l, F_0 - \lambda)$	= "kernel" in Duhamel integral in Eq. (4)

Received January 26, 1970; revision received April 27, 1970. This work was performed for the Thermal Technology Branch of the NASA/Manned Spacecraft Center under contract NAS9-8166.

\* Staff Engineer, Thermodynamics Department.

- $k$  = thermal conductivity, Btu/sec-ft-°F  
 $l$  = thickness of insulation = bondline depth, ft  
 $\dot{q}$  = constant heat rate per unit area, Btu/sec-ft<sup>2</sup>  
 $T$  = temperature, °F;  $T_i$  = constant and uniform initial temperature of two-layer slab prior to imposed heating, °F  
 $T_s$  = temperature at outer surface of insulation for  $F_0 > 0$ , °F  
 $T(l, F_0)$  = time-dependent temperature at  $l$ , °F  
 $T(l, 0)$  = initial temperature in-depth at  $x = l$ ;  $T(l, 0) = 0$  when used in Duhamel's integral, °F  
 $x$  = unidirectional depth variable for the slab (Fig. 1), ft  
 $\alpha$  = thermal diffusivity,  $k_1/\rho_1 c_{p1}$   
 $\beta_i$  = eigenvalues determined by  $\beta_i \tan \beta_i = 1/\eta$ , rad<sup>3</sup>  
 $\delta$  = thickness of backup structure, ft  
 $\epsilon$  = total hemispherical emittance of surface ( $x = 0$ )  
 $\eta$  = thermal capacitance ratio,  $(\rho \delta c_p)_2/(\rho l c_p)_1$   
 $\theta$  = time, sec;  $\theta_f$  = final time, sec  
 $\lambda$  = a dimensionless dummy time variable for which the product in Eq. (4) integral will vanish for all values of  $\lambda$  greater than  $F_0$   
 $\rho$  = density, lb/ft<sup>3</sup>  
 $\sigma$  = Stefan-Boltzmann constant,  $0.478 \times 10^{-12}$  Btu/sec-ft<sup>2</sup>-°R<sup>4</sup>

### Subscript

- 1,2 = insulation layer and backup structure, respectively

### Introduction

WELL insulated, nonreceding thermal protection systems on entry vehicles will experience aerodynamic heating during Earth entry which can result in near-equilibrium insulation outer surface temperatures. The maximum permissible temperature at the bondline between the insulation and the backup structure (Fig. 1) strongly influences the choices of materials for insulation and backup structure.

This Note presents a graphical procedure through which the bondline temperature history can be obtained when the outer surface equilibrium temperature history is known. The procedure employs a graphical representation of the "kernel" in Duhamel's integral.<sup>1</sup> (The derivation of the convolution integral (Duhamel's) and a discussion of the utility of the superposition principle for solving linear problems are available in advanced mathematics books, e.g., Ref. 2). A numerical example is given, and the results are compared with those obtainable from a closed-form solution and a solution obtained by constructing a detailed mathematical model.

### Mathematical Formulation

A number of articles<sup>3-6</sup> have been published which provide a method for obtaining the outer surface and in-depth temperature history for a two-layer slab for a sudden increase of the temperature of a fluid at the outer boundary. Grover and Holter<sup>3</sup> discuss a solution designed to accommodate zero outer surface boundary resistance and a  $k_2 \rightarrow \infty$ ; whereas, other authors<sup>4,5</sup> include a boundary resistance or a pre-

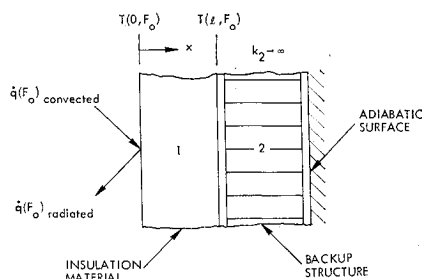


Fig. 1 Model of configuration.

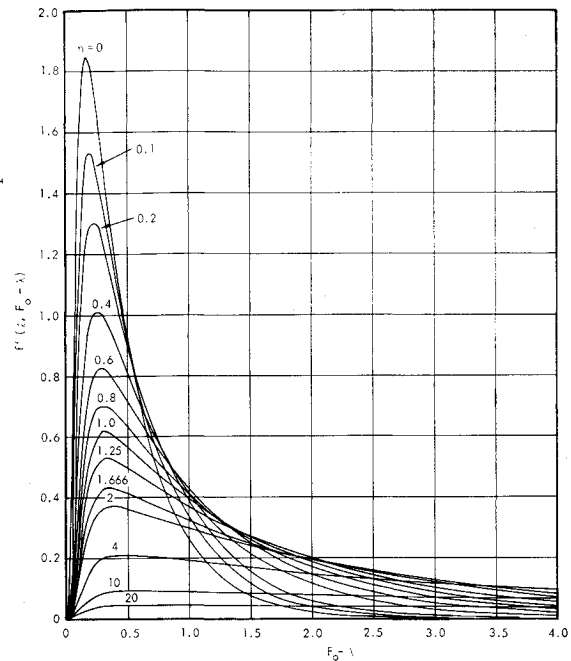


Fig. 2 The Kernel of Duhamel's integral ( $\eta$  curves).

scribed  $T_s$  in conjunction with a thermal gradient through the backup structure. Grover and Holter<sup>3</sup> also provide an equation for determining the bondline temperature, i.e., a specific solution which gives  $T(l, F_0)$  when the outer surface experiences a  $T_s$  for a given duration. Their Eq. (12)<sup>3</sup> has the following form when the outer boundary resistance equals zero and  $x = l$

$$\frac{T_s - T(l, F_0)}{T_s - T(l, 0)} = \sum_{i=1}^{\infty} \frac{2(1 + \eta^2 \beta_i^2) e^{-\beta_i^2 F_0} \cos \beta_i}{\eta \beta_i^2 (1 + \eta + \eta^2 \beta_i^2)} \quad (1)$$

The solution to Eq. (1) will provide the bondline or backup structure transient temperature (for  $k_2 \rightarrow \infty$ ) when  $T_s$ ,  $T(l, 0)$ , and the constant thermophysical properties of each material are known.

Equation (1) is useful for obtaining  $T(l, F_0)$  due to a transient temperature occurring at the exposed surface ( $x = 0$ ) by using the Duhamel integral.<sup>7</sup> To quote,<sup>7</sup> "If  $f(x, \theta)$  is the solution for the temperature history in a solid whose initial temperature is zero, and whose surface is maintained at a temperature of unity, then the solution  $v(x, \theta)$  is given by

$$v(l, F_0) = \int_0^{F_0} T_s(0, \lambda) f'(l, F_0 - \lambda) d\lambda \quad (2)$$

Equation (2) is in a slightly altered form from that used in Ref. 7. With  $T(l, F_0) = f(l, F_0)$ , Eq. (1) becomes, after setting  $T(l, 0) = 0$ ,  $T_s$  equal to unity and rearranging terms,

$$f(l, F_0) = 1 - \sum_{i=1}^{\infty} \frac{2(1 + \eta^2 \beta_i^2) e^{-\beta_i^2 F_0} \cos \beta_i}{\eta \beta_i^2 (1 + \eta + \eta^2 \beta_i^2)} \quad (3)$$

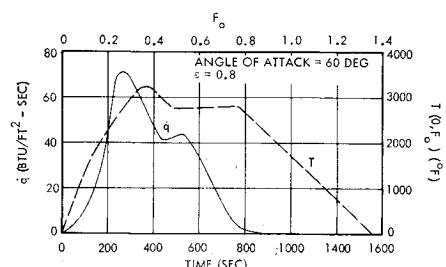


Fig. 3 Heat flux and surface temperature vs time curve.

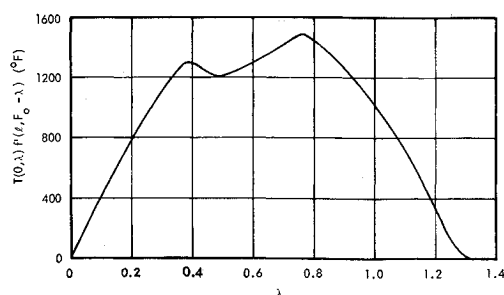


Fig. 4 Dimensionless dummy time variable vs Duhamel's integrand.

By substituting  $(F_0 - \lambda)$  for  $F_0$ , differentiating  $f(l, F_0)$  with respect to time  $F_0$ , and adding the initial temperature  $T_i$ , the bondline temperature is obtained

$$T(l, F_0) = T_i + \int_0^{F_0} T_s(0, \lambda) \times \sum_{i=1}^{\infty} \left[ \frac{2(1 + \eta^2 \beta_i^2) e^{-\beta_i^2 (F_0 - \lambda)} \cos \beta_i}{\eta(1 + \eta + \eta^2 \beta_i^2)} \right] d\lambda \quad (4)$$

The "kernel" [the summation of the bracketed term in Eq. (4)] is designated  $f'(l, F_0 - \lambda)$  and is plotted vs  $F_0 - \lambda$  for a wide range of  $\eta$  values in Fig. 2. It was evaluated with TRW's conversational on-line computer. The eigenvalues  $\beta_i$ , which are obtained by solving the equation  $\beta_i \tan \beta_i = (1/\eta)$ ,<sup>3</sup> are tabulated in Refs. 1 and 8.

#### Numerical Example

To assess the ability to predict  $T(l, F_{0f})$  for a given heating period ( $F_{0f}$ ) from a curve in Fig. 2 for a given  $\eta$ , the following numerical example was chosen. The solid curve in Fig. 3 is a typical heating rate history for a surface entering the atmosphere at an angle of attack equal to  $60^\circ$ . The dashed curve in Fig. 3 shows the corresponding outer surface temperature  $T(0, F_0)$  history, obtained by performing a radiation equilibrium thermal balance at  $x = 0$ , using the Stefan-Boltzmann equation  $q = \sigma \epsilon (T + 460)^4$  to obtain  $T$  vs  $F_0$  when  $q$  vs  $\theta$  is given. For  $F_0 = 0$  or any other time at which  $q = 0$ , the equilibrium temperature is chosen to be zero. For our example,  $T_i = 0^\circ\text{F}$ ,  $\theta_f = 950$  sec,  $k = 14.4 \cdot 10^{-4}$  Btu/sec-ft- $^\circ\text{F}$ ,  $\rho_1 = 1.0$  lb/ft<sup>3</sup>,  $c_{p1} = 1.0$  Btu/lb- $^\circ\text{F}$ ,  $\epsilon = 0.8$ ,  $l = 0.1$  ft and  $\eta = 1.0$ . The following procedure is used to obtain a bondline temperature at any  $T(l, F_{0f})$ .

1) From the dashed curve of Fig. 3, tabulate  $F_0(\lambda)$  and  $T(0, \lambda)$ , as in columns 1 and 2 on Table 1, from  $F_0 = 0$  to  $F_0 = F_{0f}$ , the time at which the bondline temperature is desired.

2) In column 3 opposite  $F_0(\lambda) = 0$ , place the value  $F_{0f}$ , since  $F_{0f} - \lambda = 1.36 - 0 = 1.36$ . Let  $F_0 = \lambda$  in column 1 and for each successive row subtract  $\lambda$  from  $F_{0f}$  to obtain the values given in column 3.

3) From Fig. 2, for  $\eta = 1.0$ , obtain the  $f'(l, F_0 - \lambda)$  values that correspond to the  $F_{0f} - \lambda$  values of column 3, and enter them in column 4.

4) In column 5, enter the products of the values in columns 2 and 4, and plot these products vs  $\lambda$ , as in Fig. 4. The area under this curve yields  $T(l, F_{0f})$ .

For the numerical example, the area under the curve of Fig. 4 is 15.66 blocks, where a block is the equivalent of  $0.2 \times 400^\circ\text{F} = 80^\circ\text{F}$ , so that the temperature for  $F_{0f} = 1.36$  is  $80^\circ\text{F} \times 15.66 = 1252^\circ\text{F}$ . Verification of this result was obtained by constructing a mathematical model with the identical thermophysical properties and boundary condition and programming the problem for solution on the TRW SINDA thermal analyzer. The SINDA computer program gave 1259.9 $^\circ\text{F}$  at 950 sec. A closed-form solution of the integral in Eq. (4), which used a half-range Fourier cosine series to define  $T(0, \lambda)$  as a continuous function, gave 1258 $^\circ\text{F}$ .

The example solution required approximately 45 min. to plot the  $T$  vs  $F_0$  curve from the  $q$  vs  $\theta$  curve, to tabulate data as on Table 1, and to obtain the area under the curve from Fig. 4 by use of a planimeter. Practice will shorten this time.

#### Discussion

The curve for  $\eta = 0$  shown on Fig. 2 was obtained from a previous work.<sup>9</sup> The eigenvalues for the  $\eta = 0$  (adiabatic bondline) problem are 1, 3, 5, ... and the kernel for Duhamel's integral was obtained from Ref. 7 and solved in a similar manner as the solution for the present investigation.

The use of Duhamel's integral appears to be restrictive, in that the initial temperature  $T(0, \lambda)$  must be zero. An equilibrium heat balance using the Stefan-Boltzmann equation for  $q = 0$  will give  $T = -460^\circ\text{F}$ , which is a trivial solution. This answer is incorrect, and an assumed value of  $0^\circ\text{F}$  for  $q = 0$  will provide accurate results. To use Duhamel's integral, one must set  $T(l, 0) = 0$ , and  $T(0, F_0)$  must be unity ( $1^\circ\text{F}$ ). This does not mean to imply that the solution works only for problems in which the composite slab temperature is uniform at zero. It is only a requirement for applying the convolution integral.

The insulation thickness required to achieve an allowable bondline limit temperature is obtained by plotting  $l$  vs  $T(l, F_0)$  for a range of  $F_{0f}$ 's. Since the  $\alpha$  and  $\theta_f$  of interest remain constant within the  $F_{0f}$ , only the value of  $l$  need be varied. Although  $\alpha$  is normally temperature-dependent, it must be considered constant for use in this solution. By selecting a realistic range of  $\alpha$ 's, both maximum and minimum, a maximum and minimum insulation material thickness can be determined for a given trajectory. The combination of radiation equilibrium temperature at the outer surface and a maximum  $\alpha$  corresponding to the highest expected temperature will provide very conservative results.

The basic equation from Ref. 3 contains  $x$  as a variable. For this analysis,  $x$  was set equal to  $l$ , the bondline position. Should data for other in-depth positions be required, the basic equation can be altered to accommodate this new requirement and Duhamel's integral solved with another set of  $\eta$  curves.

There is significance to the shape of the  $\eta$  curves on Fig. 2 for very small  $\eta$  values. For  $\eta = 0, 0.1$ , and  $0.2$  problems in which the  $(F_{0f} - \lambda) > 3.0, 3.2$ , and  $3.6$ , respectively, there will be negligible contribution to the temperature rise at the bondline due to  $f'(l, F_0 - \lambda) \rightarrow 0$  as  $F_{0f} - \lambda$  exceeds the values noted. For  $F_{0f} - \lambda \rightarrow 0$ , there will be a negligible temperature change at the bondline, regardless of the magnitude of  $T(0, \lambda)$ .

It should be noted that this solution is applicable only to two-layer slabs which are flat or have a large radius of curva-

Table 1 Tabulation for the "numerical example" ( $\eta = 1$ )

(1) $F_0(\lambda)$	(2) $T(0, \lambda)$	(3) $F_{0f} - \lambda$	(4) $f'(l, F_0 - \lambda)$	(5) = (2) $\times$ (4)
0	0	1.36	0.303	0
0.1	1325	1.26	0.327	433
0.2	2250	1.16	0.352	791
0.3	2950	1.06	0.380	1120
0.38	3240	0.98	0.402	1303
0.4	3160	0.96	0.410	1297
0.487	2760	0.873	0.438	1209
0.6	2775	0.76	0.470	1303
0.7	2800	0.66	0.507	1420
0.760	2820	0.60	0.530	1493
0.8	2660	0.56	0.545	1450
0.9	2180	0.46	0.582	1270
1.0	1700	0.36	0.609	1035
1.103	1215	0.257	0.595	723
1.2	755	0.16	0.435	328
1.3	290	0.06	0.035	10
1.36( $F_{0f}$ )	0	0	0	0

ture. Wing leading edges made of two materials, but with small radii, require a solution of the diffusion equation in cylindrical coordinates. The presented  $\eta$  curves may be used for a leading edge problem, but the bondline temperature obtained would be lower by an unknown amount than would actually be experienced with a more nearly exact solution using cylindrical coordinates.

### References

- <sup>1</sup> Harris, H. J., "A Graphical Method for Obtaining the Transient Bondline Temperature for Two Finite Composite Slabs Subjected to Aerodynamic Heating," IOC 69.4352.8-22, Dec. 1969, TRW Systems Group, Houston, Texas.
- <sup>2</sup> Churchill, R. V., *Operational Mathematics*, McGraw-Hill, New York, 1958, pp. 38-40, 229-231.
- <sup>3</sup> Grover, J. H. and Holter, W. H., "Solution of the Transient Heat-Conduction Equation for an Insulated, Infinite Metal Slab," *Jet Propulsion*, Vol. 27, No. 12, Dec. 1957, pp. 1249-1252.
- <sup>4</sup> Mayer, E., "Heat Flow in Composite Slabs," *ARS Journal*, Vol. 22, No. 3, May-June 1952, pp. 150-158.
- <sup>5</sup> Harris, R. S., Jr. and Davidson, J. R., "An Analysis of Exact and Approximate Equations for the Temperature Distribution in an Insulated Thick Skin Subjected to Aerodynamic Heating," TN D-519, Jan. 1961, NASA.
- <sup>6</sup> Grover, J. H. and Holter, W. H., "Insulation Temperature for the Transient Heating of an Insulated Infinite Metal Slab," *Journal of the American Rocket Society*, Vol. 30, No. 9, Sept. 1960, pp. 907-908.
- <sup>7</sup> Schneider, P. J., *Conduction Heat Transfer*, Addison-Wesley, Reading, Mass., Sept. 1957, pp. 272-273, 235-236.
- <sup>8</sup> Abramowitz, M. and Stegun, I. A., *Handbook of Mathematical Functions with Formulas, Graphs, and Mathematical Tables*, National Bureau of Standards Applied Mathematics Series 55, June 1964, p. 225.
- <sup>9</sup> "Derivation of Duhamel Method for Calculating Back Face Temperatures," General Dynamics Corp., Fort Worth, Texas, 1960.

## Fundamental Sloshing Frequency for an Inclined, Fluid-Filled Right Circular Cylinder

W. A. McNEILL\*

University of South Alabama, Mobile, Ala.

AND

J. P. LAMB†

The University of Texas at Austin, Austin, Texas

### Nomenclature

- $a_k^m$  =  $k$ th constant in expansion for  $\psi_m$   
 $F$  = frequency parameter,  $\omega^2 R/g$   
 $g$  = gravitational acceleration  
 $h$  = depth of fluid in container (Fig. 1)  
 $I_{ij} = \int_0^{2\pi} (\cos\theta)^L (\sin\theta)^J d\theta$   
 $L = m + p - k - q$ , where  $m, p, k, q$  are summation indices  
 $N$  = number of terms in expansion for  $\varphi$   
 $n$  = outward normal to surface bounding fluid  
 $R$  = radius of container

Received February 13, 1970. This work was conducted in part at Marshall Space Flight Center under a 1969 Summer Faculty Fellowship Program, sponsored by NASA and the American Society for Engineering Education.

\* Assistant Professor of Mechanical Engineering.

† Associate Professor of Mechanical Engineering. Member AIAA.

- $r, z$  = radial and longitudinal coordinates (Fig. 1)  
 $S$  = undisturbed free surface of fluid  
 $t$  = time  
 $\alpha_m$  =  $m$ th constant in expansion for  $\varphi$   
 $\theta$  = angular coordinate (Fig. 1)  
 $\rho$  = fluid density  
 $\tau$  = region containing fluid  
 $\phi$  = angle of inclination (Fig. 1)  
 $\varphi$  = velocity potential  
 $\psi_m$  =  $m$ th function in expansion for  $\varphi$   
 $\omega$  = fundamental sloshing frequency

**S**TUDIES<sup>1,2</sup> of the natural sloshing frequencies of incompressible fluids have found important applications in the design of space flight vehicles. Previous investigations have been restricted to cases where the container was vertically aligned with the Earth's gravitational field. However, with increasing attention being directed toward the design of shuttle vehicles operating between Earth and orbiting platforms, it becomes necessary to consider the problem of the behavior of fuel in a tank which is inclined to the Earth's gravitational field. The present Note demonstrates how the variational principle first employed by Lawrence, Wang, and Reddy<sup>3</sup> can be used to compute the fundamental frequency of oscillation of a liquid in an arbitrarily inclined container.

The fluid is assumed to be incompressible and inviscid, and the tank is considered to be rigid. The governing equations for small oscillations under these restrictions are as follows:<sup>2</sup> Within the fluid region the velocity potential  $\varphi$  must satisfy the Laplace equation

$$\nabla^2 \varphi = 0 \quad (1)$$

while, on the wetted surface,

$$\partial \varphi / \partial n = 0 \quad (2)$$

whereas, on the undisturbed free surface of the liquid,

$$\partial \varphi / \partial n + (1/g) \partial^2 \varphi / \partial t^2 = 0 \quad (3)$$

It has been shown<sup>3</sup> that the function  $\varphi$  which extremizes the integral

$$J = \frac{1}{2} \rho \int_{t_1}^{t_2} \left[ \int_{\tau} \nabla \varphi \cdot \nabla \varphi d\tau - \left( \frac{1}{g} \right) \int_S \left( \frac{\partial \varphi}{\partial t} \right)^2 dS \right] dt \quad (4)$$

must also satisfy Eqs. (1-3).

Rattayya<sup>4</sup> has employed a series expansion of  $\varphi$  in terms of harmonic polynomial functions to extremize the integral Eq. (4) and thus obtain the natural frequencies of liquid oscillation in a vertical axisymmetric ellipsoidal tank. His approach is modified here to obtain solutions for the case of a skewed cylinder.

Using the coordinate system of Fig. 1, the limits of the

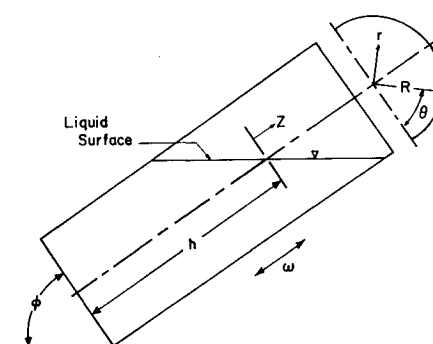


Fig. 1 Schematic of inclined fluid-filled cylinder.